Supporting Information for:

Strong Magnetic Exchange Coupling in the Cyano-Bridged Coordination Clusters $[(PY5Me_2)_4V_4M(CN)_6]^{5+}$ (M = Cr, Mo)

Danna E. Freedman, David M. Jenkins and Jeffrey R. Long

Department of Chemistry, University of California, Berkeley, California 94720-1460

Chem. Commun.

Additional Experimental Details

Mass Spectrometry. Electrospray ionization mass spectra were acquired in positive ion mode using a quadrupole time-of-flight (Q-Tof) mass spectrometer equipped with a Z-spray electrospray ionization (ESI) source (Q-Tof Premier™, Waters, Milford, MA). Sample solutions were withdrawn from glass vials capped with rubber septa using a 250 μL Gastight® syringe (Hamilton, Reno, NV) and immediately infused into the ESI probe at flow rates of 6 to 10 μL/min using a syringe pump. Charged droplets of the sample solution were emitted from a stainless steel capillary (inner diameter 127 μm) with nitrogen nebulizing gas flow of 800 L/hr. Typical instrument parameters were as follows: capillary voltage 0.2 to 3.5 kV, sample cone 10 to 180 V, extraction cone 3 V, ion guide 1 V, source block temperature 80 ºC, desolvation (nebulizing) gas temperature 150 ºC, accelerating voltage into the argon-filled cell 4 V, first pumping stage pressure 1.5 mbar, ion transfer stage pressure 6×10^{-4} mbar, quadrupole analyzer pressure 2×10^{-5} mbar, argon-filled cell pressure 8×10^{-3} mbar, Tof analyzer pressure 9×10^{-7} mbar. No cone gas flow was used. For each sample, the sample cone and extraction cone voltages were adjusted to optimize signal for the ion(s) of interest, and the ESI capillary voltage was adjusted to maintain ion counts below the dead-time threshold (< 0.1 ions per push) to prevent spectral distortion effects due to detector saturation. The Tof analyzer was operated in "V" mode. Under these conditions, a mass resolving power, R, of 1.0×10^4 was routinely achieved, where $R = m/\Delta m_{50\%}$, m is the mass-to-charge ratio of an ion, and $\Delta m_{50\%}$ is the full width of the mass spectral peak at half-maximum height.[1] This was more than sufficient to resolve the isotopic distributions of the singly and multiply charged ions measured in this study. Thus, an ion's mass and charge could be determined independently, i.e., an ion's charge state can be determined from the reciprocal of the spacing between adjacent isotope peaks in the m/z spectrum. External mass calibration was performed using solutions of sodium formate or sodium iodide immediately prior to measuring samples. Mass spectra were processed using MassLynx software (version 4.1, Waters).

X-ray Structure Determinations. X-ray diffraction measurements were performed on single crystals coated with Paratone oil and mounted on Kaptan loops. Each crystal was frozen under a stream of N_2 while data were collected on a Bruker APEX diffractometer. A matrix scan

using at least 20 centered reflections was used to determine initial lattice parameters. Reflections were merged and corrected for Lorenz and polarization effects, scan speed, and background using SAINT 4.05. Absorption corrections, including odd and even ordered spherical harmonics were performed using SADABS. Space group assignments were based upon systematic absences, *E* statistics, and successful refinement of the structures. Structures were solved by Patterson maps with the aid of successive difference Fourier maps, and were refined against all data using the SHELXTL 5.0 software package. Hydrogen atoms were assigned to ideal positions and refined using a riding model with an isotropic thermal parameter 1.2 times that of the attached carbon atom (1.5 times for methyl hydrogens). Hydrogen atoms were not added for solvent molecules. Not all fluorine atoms on the counter ions could be located. Chemically we assume they are all present. This solvent disorder was modeled by assuming partially occupied solvent molecules which appear to be bonded together. It is important to note that the molecules do not occupy the same space at the same time, they are spatially disordered. In the case of many solvent molecules we believe that only a small part of an acetonitrile is sufficiently ordered to be observed. There are several solvent molecules which are only partially modeled in this method.

Magnetic Measurements. Magnetic data were collected using a Quantum Design MPMS-XL SQUID magnetometer. DC magnetic susceptibility data were collected at temperatures ranging from 5 to 300 K, and at fields of 0.1, 0.5, 1, and 5 T. Magnetization data were collected at applied fields of 1, 2, 3, 4, 5, 6, and 7 T at temperatures ranging from 1.8 to 10 K. AC magnetic susceptibility measurements were performed in zero applied field using a switching field of 4 G at temperatures from 1.8 to 10 K. Measurements were performed on samples sealed in quartz tubes under vacuum. Frozen diethyl ether was used as a restraint to prevent torquing. Data were fit with Magfit3.0 which uses the Van Vleck equation.

Other Physical Measurements. Infrared spectra were collected on a Nicolet Avatar 360 FTIR spectrometer with an attenuated total reflectance accessory. Carbon, hydrogen, and nitrogen analyses were obtained from the Microanalytical Laboratory of the University of California, Berkeley.

Reference

(1) Marshall, A.G.; Hendrickson, C.L.; Jackson, G.S. *Mass Spectrom. Rev.* **1998**, *17*, 1-35.

Table S1. Crystallographic Data[a] for Compounds **1′** and **2′**

identification	**1′**	**2′**
Formula	$C_{137}H_{100}F_{30}V_4N_{33}O_1P_5Cr$	$C_{135}H_{100}F_{30}V_4N_{33}O_{0.5}P_5Mo$
FW	3183.6	3179.03
T, K	156 (2)	140 (2)
cryst. syst., space group	Tetragonal, *I4/mcm*	Tetragonal, *I4/mcm*
Z	8	8
a, Å	33.307 (1)	33.492(2)
b, Å	33.307 (1)	33.492(2)
c, Å	28.889 (2)	29.015(4)
α,β,γ °	90.00(0)	90.00(0)
V, Å^3	32048.63	32546(5)
d_{calc}, g/cm^3	1.321	1.298
abs. coeff. mm^{-1}	0.43	0.432
data / restr. / param.	6071 / 0 / 493	5259 / 0 / 464
GOF on F^2	2.675	2.041
R_1 (wR_2), %, [I>2sigma(I)][b]	0.0989 (0.2882)	0.0954 (0.2711)
R_1 (wR_2), %, all data	0.1237 (0.3159)	0.1317 (0.2883)

[a]Obtained with graphite-monochromated Mo Kα (λ = 0.71073 Å) radiation.
[b]$R_1 = \Sigma||F_o| - |F_c||/\Sigma|F_o|$, $wR_2 = \{\Sigma[w(F_o^2-F_c^2)^2]/\Sigma[w(F_o^2)^2]\}^{1/2}$.

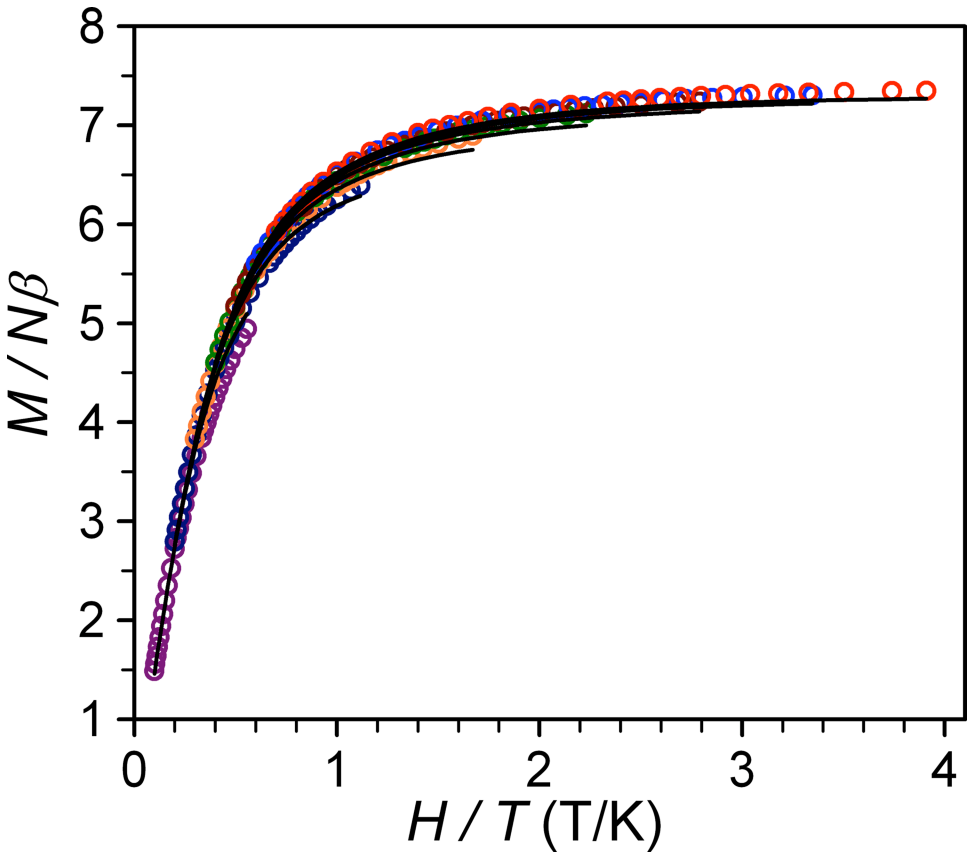

Figure S1. Low-temperature magnetization data for **1** collected in applied fields of 1 (purple), 2 (darkblue), 3 (orange), 4 (green), 5 (maroon), 6 (blue), and 7 (red) T. The solid lines represent fits to the data.

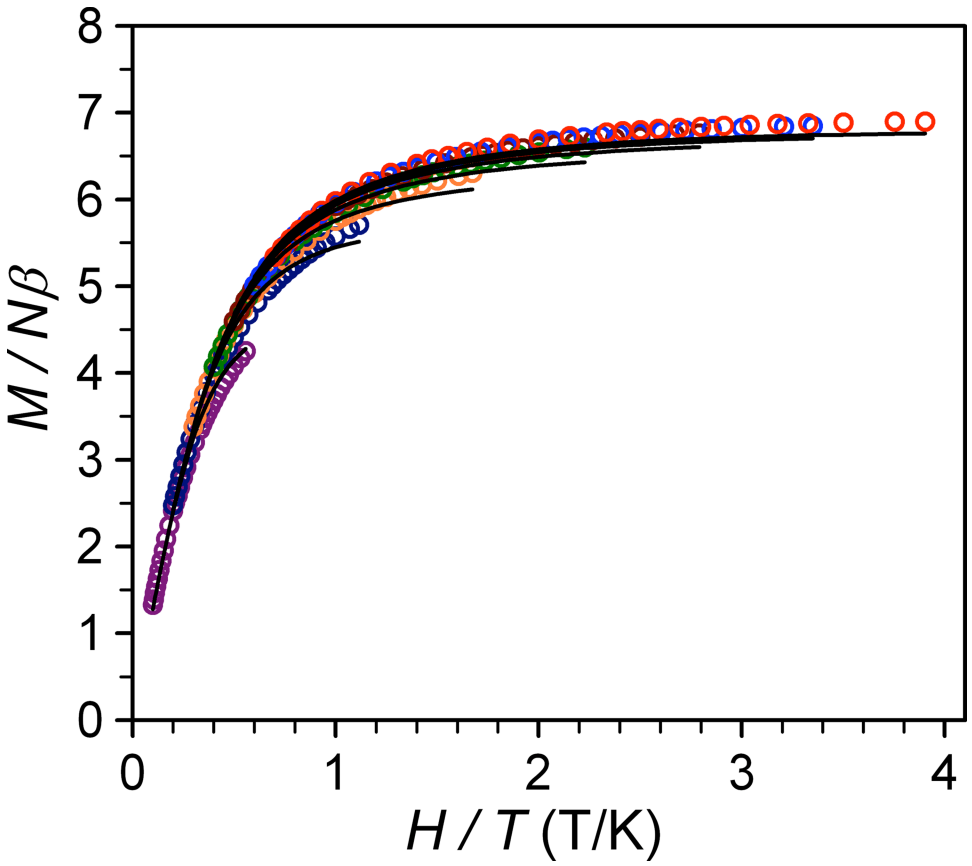

Figure S2. Low-temperature magnetization data for **2** collected in applied fields of 1 (purple), 2 (dark blue), 3 (orange), 4 (green), 5 (maroon), 6 (blue), and 7 (red) T. The solid lines represent fits to the data.

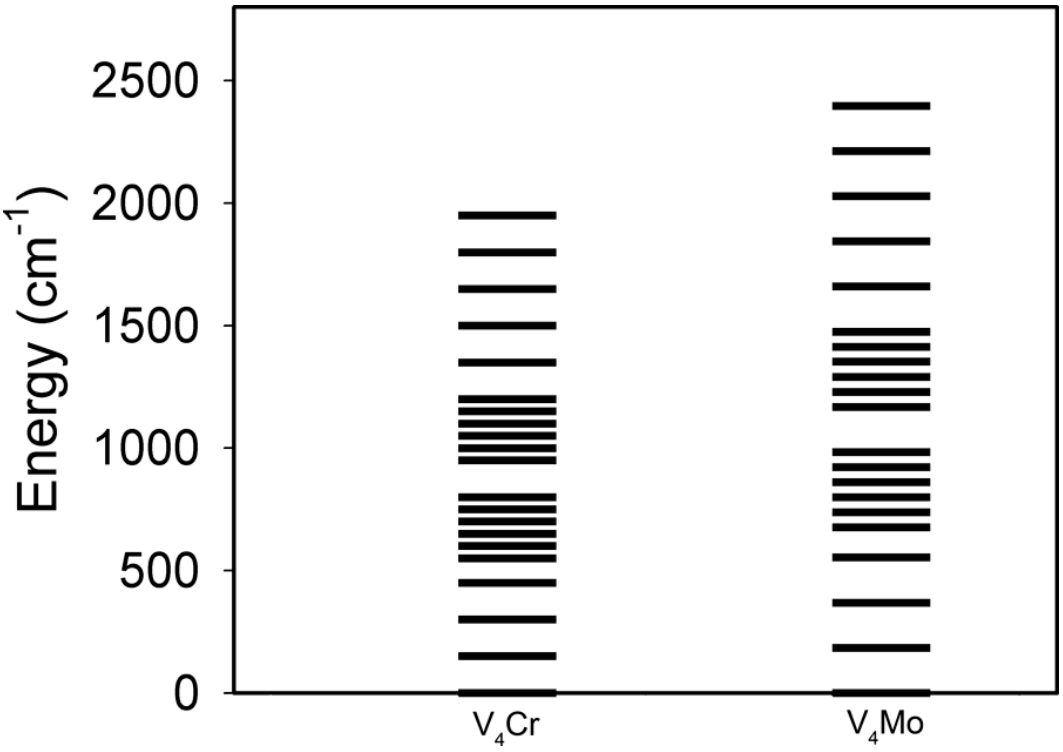

Figure S3. Spin ladder for V_4Cr and V_4Mo showing all energy levels.

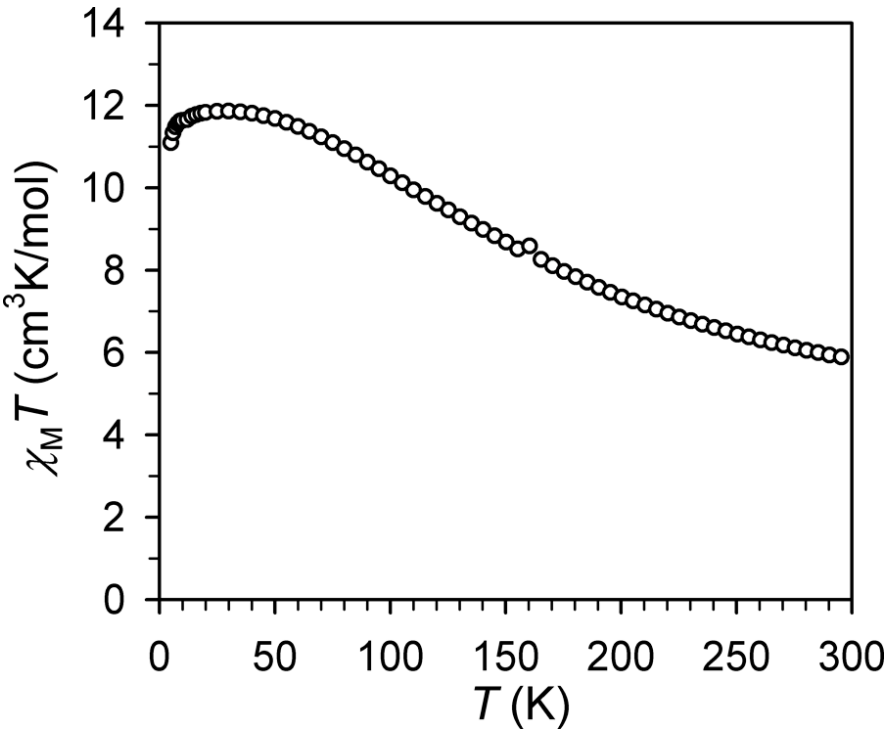

Figure S4. Magnetic susceptibility data for V_4Cr taken at 1000 Oe. This data demonstrates that the downturn is significantly reduced at lower field.

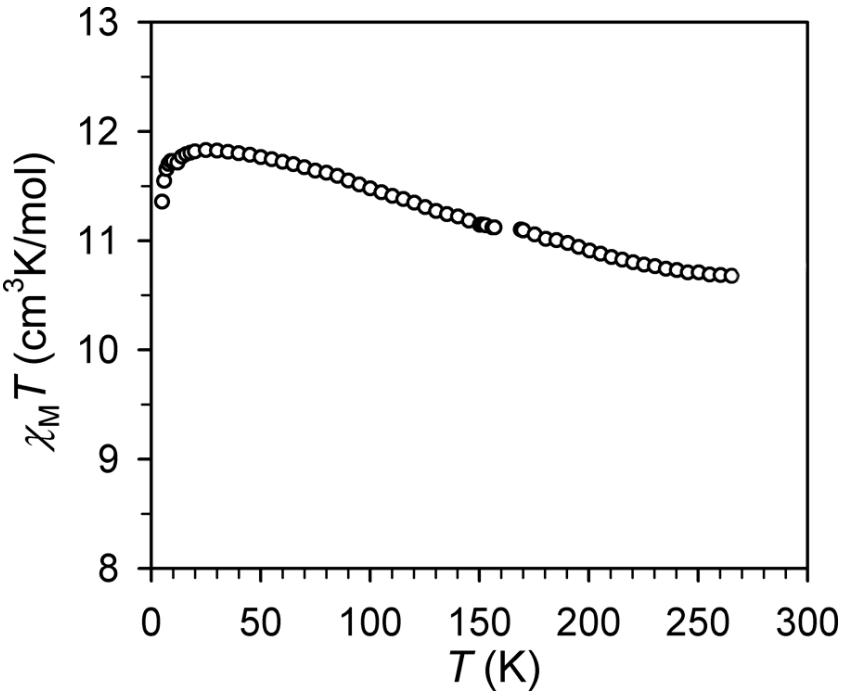

Figure S5. Magnetic susceptibility data for V_4Mo taken at 1000 Oe. This data demonstrates that the downturn is significantly reduced at lower field. The gap at 160 K is due to the diethyl ether used as a physical restraint. The diethyl ether causes several unusable data points at its melting point.